Quantitative Description of Sodium and Potassium Currents and Computed Action Potentials in *Myxicola* Giant Axons

L. GOLDMAN and C. L. SCHAUF

From the Department of Physiology, School of Medicine, University of Maryland, Baltimore, Maryland 21201. Dr. Schauf's present address is Department of Neurological Science, Rush-Presbyterian-St. Luke's Medical Center, Chicago, Illinois 60612.

ABSTRACT An analysis of the sodium and potassium conductances of *Myxicola* giant axons was made in terms of the Hodgkin-Huxley m, n, and h variables. The potassium conductance is proportional to n^2. In the presence of conditioning hyperpolarization, the delayed current translates to the right along the time axis. When this effect was about saturated, the potassium conductance was proportional to n^3. The sodium conductance was described by assuming it proportional to m^3h. There is a range of potentials for which τ_h and h_∞ values fitted to the decay of the sodium conductance may be compared to those determined from the effects of conditioning pulses. τ_h values determined by the two methods do not agree. A comparison of h_∞ values determined by the two methods indicated that the inactivation of the sodium current is not governed by the Hodgkin-Huxley h variable. Computer simulations show that action potentials, threshold, and subthreshold behavior could be accounted for without reference to data on the effects of initial conditions. However, recovery phenomena (refractoriness, repetitive discharges) could be accounted for only by reference to such data. It was concluded that the sodium conductance is not governed by the product of two independent first order variables.

INTRODUCTION

In their description of membrane currents in squid axons, Hodgkin and Huxley (1952 *c*) accounted for the inactivation of the sodium current by supposing that the relatively slow exponential decay of this current that is observed during a depolarizing step in potential could simply be extrapolated to the beginning of the step. In this way they defined first order independent activation (m) and inactivation (h) variables. An alternative point of view, also proposed by them and developed by Hoyt (1963), is to suppose that the sodium conductance is governed by a single, second order variable, i.e. that the activation and inactivation processes are coupled.

A considerable array of experimental data can be accounted for equally well by assuming either coupled or independent models for the sodium conductance (Hodgkin and Huxley, 1952 *c*; Hoyt, 1963, 1968). However, there are available a number of observations which are inconsistent with independent activation and inactivation kinetics as proposed by Hodgkin and Huxley. In *Myxicola* axons, the steady-state inactivation curve was found to depend on the sodium conductance during the test pulse used for the determination, translating to the right about 6 mV for a twofold increase in conductance (Goldman and Schauf, 1972). This is the sort of behavior expected for a coupled system (Hoyt, 1968). A dependency of the steady-state inactivation curve on the test pulse was also reported in squid (Hoyt and Adelman, 1970), and probably accounts for at least some of the variability in inactivation curves in the node seen by Frankenhaeuser (1959). In *Dosidicus* axons (Armstrong, 1970) and in *Myxicola* (Goldman and Schauf, 1972) there is a delay in the development of inactivation which depends in some way on the time taken for the rise of the sodium conductance during the conditioning pulse (Goldman and Schauf, 1972). A way to summarize these observations is to note that measured values of the inactivation state are a function of the activation state. This suggests that activation and inactivation are not independent, but coupled. However, other interpretations are also possible.

There is another test of Hodgkin–Huxley kinetics that can be made. If the sodium conductance really is governed by independent m and h variables, then one can study the inactivation process in the manner described by Hodgkin and Huxley (1952 *b*) by examining the effects of conditioning voltages of various durations on the peak sodium current produced by a fixed test pulse. For Hodgkin-Huxley kinetics the time constant of the curve relating the peaks of the sodium currents during successive test pulses to the duration of the conditioning pulse at some potential should be identical to the time constant of decay of the sodium current during a continuous pulse at that same potential. For coupled activation-inactivation kinetics the two time constants are not required to be the same.

In an earlier report (Goldman and Schauf, 1972) we described inactivation characteristics of the sodium current in *Myxicola* as determined by the effects of conditioning pulses. We present here observations on inactivation in *Myxicola* as determined from the decay of the sodium current during a potential step. Observations on the activation of the sodium current and on the potassium current are also included. All of the data of this report have been analysed exclusively in terms of the m, h, and n (for potassium) variables of Hodgkin and Huxley.

METHODS

All methods for preparing and voltage clamping *Myxicola* axons are as described by Binstock and Goldman (1969). Compensated feedback (Hodgkin, Huxley, and

Katz, 1952) was used throughout. However there will generally still be some small residual uncompensated series resistance (Goldman and Schauf, 1972).

The experimental procedure was to record membrane currents during a series of depolarizing voltage steps under fixed initial conditions. For observations on the potassium current the holding potential from which steps were made was always the resting membrane potential. For observations on the sodium current the holding potential was hyperpolarized by 50 mV for 80 ms before each voltage step. In this way m_o could be taken as zero and h_o as unity. In one experiment (triangles in Fig. 8 and filled circles in Fig. 13) this prehyperpolarization was omitted without any obvious effect on the rate constants. For experiments on sodium currents, 15 s were allowed between each depolarizing voltage-clamp step.

Sodium currents were extracted by repeating each experiment in bathing media containing 1×10^{-6} M tetrodotoxin (TTX; Calbiochem, Los Angeles, Calif.) and making a point by point in time subtraction of these currents from those in normal artificial seawater. Observations on potassium currents were also made in 1×10^{-6} M TTX. To correct potassium currents for leak the resting steady-state leak conductance, g_L, was determined and assumed to be independent of potential and time. Neither of these assumptions is in fact true, but for potassium currents there should be only little error introduced this way (Goldman and Binstock, 1969 *b*).

We have converted membrane current (I) to conductance (g) by the expression $g = I/(V - V_e)$, where V is membrane potential and V_e is an equilibrium potential. This expression makes no allowance for any changes in the conductance of the channel itself due to redistribution of the ion concentration profile with the applied field. However, the error introduced should be very small. For example, for the potassium conductance over the potential range of interest the observed changes in the steady-state value of g_K are more than 30 times greater than predicted from the constant field equation (Goldman, 1943; Hodgkin and Katz, 1949), and the shape of the normalized gating function (i.e. n_∞ (V), see below) extracted from the conductance data should be very little affected by ion redistribution in the channel. Moreover, both the peak sodium and steady-state potassium conductances do display well defined saturated values (Figs. 1 and 8).

Potentials are reported as absolute membrane potential, V (inside minus outside). Liquid junction potentials are corrected according to the values of Cole and Moore (1960 *a*; see also Binstock and Goldman, 1971). Artificial seawater had the following composition: 430 mM Na, 10 mM K, 10 mM Ca, 50 mM Mg, 560 mM Cl, 5 mM tris(hydroxymethyl)aminomethane, pH 8.0 ± 0.1. Temperature was 5° ± 1°C.

RESULTS

The Potassium Conductance

From an examination of the delayed current reversal potential as a function of the external potassium concentration, $[K]_o$, Binstock and Goldman (1971) concluded that the delayed current in *Myxicola* is carried very largely by potassium ions. We refer to the delayed current and conductance therefore as I_K and g_K, respectively. V_K was taken as −78 mV (Binstock and Goldman, 1971).

Fig. 1 shows the steady-state g_K relative to the maximum value for that axon, $\overline{g_K}$, as a function of membrane potential. Data from five axons are shown and the individual g_K values are tabulated in Table I. The solid line in Fig. 1 indicates an e-fold increase in g_K for 13 mV.

g_K as a function of potential and time (t) was analyzed as described by Hodgkin and Huxley (1952 *c*), by assuming that g_K is proportional to some power of a variable n. n can vary between 0 and 1 and is defined by

$$dn/dt = \alpha_n(1 - n) - \beta_n n, \tag{1}$$

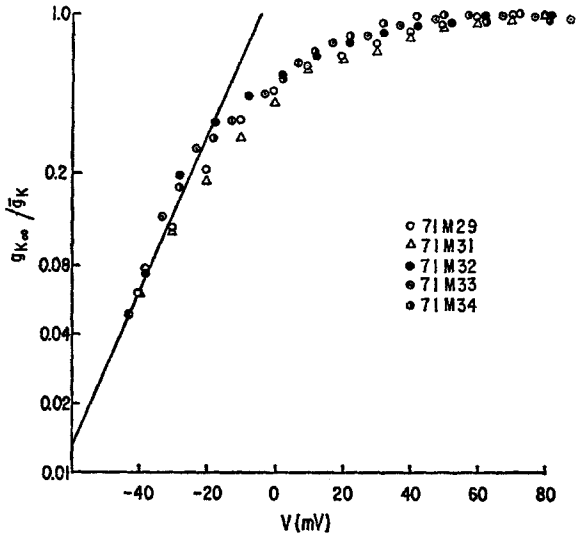

FIGURE 1. Steady-state potassium conductance, $g_{K\infty}$, relative to the maximum value in each axon, $\overline{g_K}$, as a function of membrane potential in *Myxicola*. Each symbol type represents a different axon. The solid line has been drawn to show an e-fold change in conductance for 13 mV.

where α_n and β_n are potential dependent rate constants. For *Myxicola* a power of two gave satisfactory fits.

The points in Fig. 2 are experimental values, from a single axon, of g_K as a function of time for each of the potentials indicated at the right. The solid curves, which are taken to be a good description of the points, have been computed from

$$g_K = \overline{g_K}\, n^2 \tag{2}$$

and

$$n = n_\infty - (n_\infty - n_o)e^{-t/\tau_n}. \tag{3}$$

TABLE I

VARIOUS EXPERIMENTAL VALUES USED IN THE ANALYSIS OF g_{Na} AND g_K IN *MYXICOLA* GIANT AXONS

Axon	$\overline{g_K}$	g_L	V_{Na}	$g_{Na_{max}}$	$\overline{g_{Na}}$
	mmho/cm²	*mmho/cm²*	*mV*	*mmho/cm²*	*mmho/cm²*
71M29	10.4	0.47	60	15.0	45
71M31	10.4	0.58	60	14.5	42
71M32	6.1	0.58	61	18.0	38
71M33	7.1	0.47	60	17.0	38
71M34	4.8	0.835	58	13.0	31.5
Mean	7.76	0.587	59.8	15.5	38.9

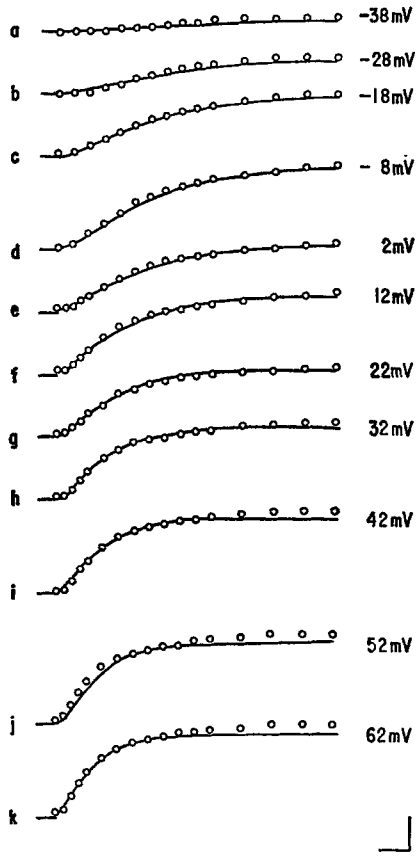

FIGURE 2. Potassium conductance as a function of time for each of the potentials indicated. The circles are experimental values and the solid lines have been computed according to $g_K = \overline{g_K} n^2$ (see text). The horizontal lines at the left indicate zero conductance, and the first circle for each curve indicates the beginning of the step. Scale: (*a*)–(*d*), 1 mmho/cm², (*e*)–(*f*), 1.5 mmho/cm², (*g*)–(*k*), 2 mmho/cm², 4 ms.

Eq. 2 is a solution of Eq. 1 for a step in potential applied at $t = 0$, where $\tau_n = 1/(\alpha_n + \beta_n)$, the steady-state value $n_\infty = \alpha_n/(\alpha_n + \beta_n)$, and n_o is the initial value. The horizontal lines at the left of each curve indicate zero conductance for reference, and the first point is at $t = 0$ in each case. The individual values used to compute each of the curves in Fig. 2 are listed in Table II.

Fig. 3 shows the collected n_∞ values, from each of the five axons analyzed, as a function of potential and in Fig. 4 the corresponding τ_n values are shown. The solid lines in Figs. 3 and 4 have been computed from Eqs. 4 and 5 below. In Fig. 5 the rate constants α_n (open circles) and β_n (filled circles) computed from the τ_n and n_∞ values are shown as functions of potential.

TABLE II

CONSTANTS USED TO COMPUTE THE g_K CURVES OF FIG. 2

V	n_∞	τ_n	α_n	β_n
mV		*ms*	ms^{-1}	ms^{-1}
−38	0.272	13.64	0.020	0.053
−28	0.445	11.26	0.040	0.049
−18	0.582	9.26	0.063	0.045
−8	0.673	8.70	0.077	0.038
2	0.746	8.11	0.092	0.031
12	0.800	6.48	0.123	0.031
22	0.850	5.67	0.150	0.026
32	0.880	4.83	0.182	0.025
42	0.900	4.35	0.207	0.023
52	0.930	3.94	0.236	0.018
62	0.940	3.50	0.269	0.017

$\overline{g_K}$ is 6.1 mmho/cm^2.

The solid curves have been drawn according to

$$\alpha_n = \frac{1}{2.85[\exp(V - 21/ - 22.8) + 1]} \tag{4}$$

and

$$\beta_n = 0.045 \exp(-V/138). \tag{5}$$

Eqs. 1, 2, 4, and 5 provide a description of g_K in *Myxicola* as a function of potential and time. n_o at a resting membrane potential of −65 mV will be 0.1.

In squid axons, conditioning hyperpolarization produces a delay in the rise of the potassium current, the I_K curves translating to the right along the time axis. This effect has been analyzed by Cole and Moore (1960 *b*) and was

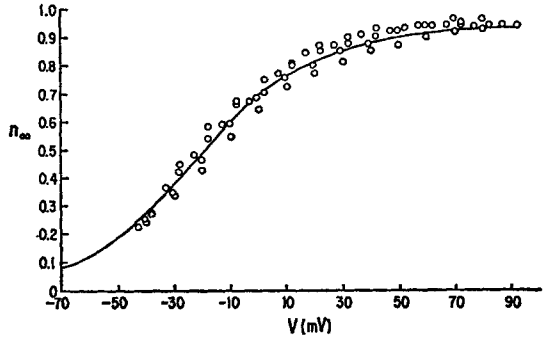

FIGURE 3

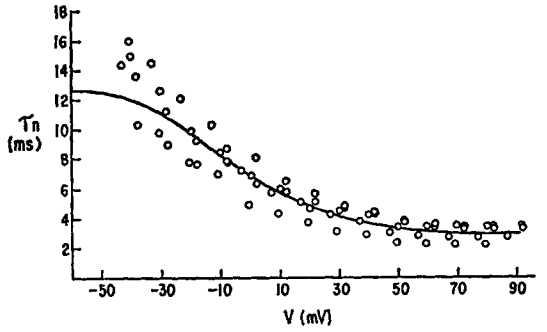

FIGURE 4

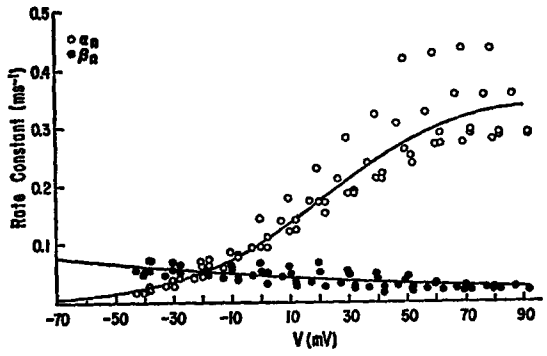

FIGURE 5

FIGURE 3. The steady-state value of the potassium conductance variable, n_∞, as a function of membrane potential. The solid curve has been computed from Eqs. 4 and 5 in the text.

FIGURE 4. The time constant of the n variable, τ_n, as a function of membrane potential. The solid curve has been computed from Eqs. 4 and 5 in the text.

FIGURE 5. The rate constants for the potassium conductance, α_n (open circles) and β_n (filled circles) as functions of membrane potential. The solid curves have been computed from Eqs. 4 (open circles) and 5 (filled circles) in the text.

also reported by Frankenhaeuser and Hodgkin (1957). The effect of the hyperpolarization is to reduce n_o. The displacement along the time axis originates from the different times needed to reach the n_o appropriate to that conditioning potential from a zero reference state (Cole and Moore, 1960 *b*).

In Fig. 6 the effects of conditioning hyperpolarization on I_K in two different *Myxicola* axons are shown. The horizontal lines at the left indicate zero current in each case. In (*a*) and (*c*), current traces in response to a step to a fixed potential, but from each of the different holding potentials (in millivolts) indicated, are seen. The two left-hand traces, labeled −60.5 and −63.5, are

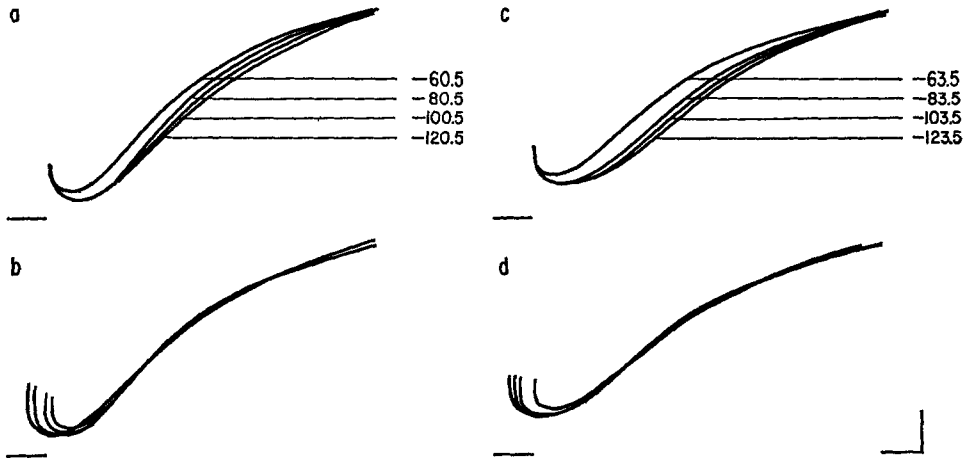

FIGURE 6. (*a*), (*c*), traces of delayed currents in two *Myxicola* axons. The potential during the step was always 69.5 mV in (*a*) and 57.5 mV in (*b*). The potential preceding the step is indicated in millivolts at the right of each trace. (*b*) and (*c*) show the same traces as (*a*) and (*c*), respectively, but translated along the time axis. The horizontal lines at the left indicate zero current. Scale: 0.15 mA/cm², 1 ms.

without conditioning pulses. Conditioning hyperpolarization does produce a delay in the rise of I_K and this is largely attributable to a simple translation along the time axis. Parts (*b*) and (*d*) of Fig. 6 show the same current traces as (*a*) and (*c*), respectively, but displaced horizontally by differing amounts. Except for the capacity and early leak currents, the translated curves superimpose. The effect seems to be about saturated for a hyperpolarization of 60 mV. An additional 60 mV of hyperpolarization to an absolute membrane potential of −180 to −190 mV produces only a negligible further displacement.

In Fig. 7 the conductance-time curves for two of the traces in Fig. 6 *c* are shown. The points are the experimental values, and the solid curves have been computed using the parameters indicated. In part (*a*) the trace without a conditioning prepulse is shown. The solid curve has been computed by

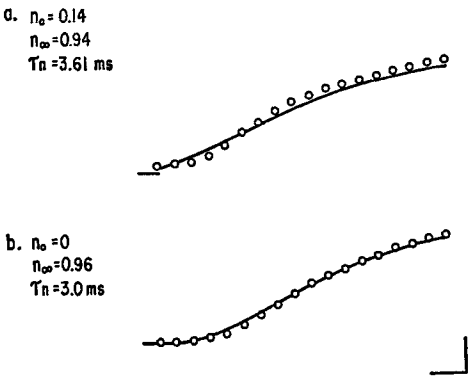

FIGURE 7. Potassium conductance as a function of time. The potential during the step was 57.5 mV. In (*a*), the holding potential was the natural resting potential. In (*b*), the step was preceded by a 60 mV hyperpolarizing potential for 80 ms. The circles are experimental values. The solid curves have been computed from (*a*) $g_K = \overline{g_K} n^2$ and (*b*) $g_K = \overline{g_K} n^3$, using the values indicated. Scale: 1.5 mmho/cm², 1 ms.

assuming g_K is proportional to n^2 as described above. Part (*b*) shows the trace with a 60 mV hyperpolarizing prepulse. The effects of conditioning hyperpolarization are then nearly maximal. This curve has been computed by assuming that g_K is proportional to n^3. n_∞ and τ_n have been slightly adjusted for best fit, and n_o is now zero. These results differ from those reported in squid in that high powers of n are not needed to account for the time-course of g_K in the presence of strong conditioning hyperpolarization (Cole and Moore, 1960 *b*).

One further comment may be made about these data. Goldman and Binstock (1969 *b*) described a rectifying early leak current voltage characteristic in *Myxicola*. This was attributed largely to a potassium component which showed constant field rectification. The n system in *Myxicola* shows constant field rectification (Binstock and Goldman, 1971). However the rectification in the early leak described by Goldman and Binstock cannot originate entirely in the n system, as it was still observed when conditioning hyperpolarizations of 40 mV were given. The data of Fig. 6 confirm that at the times for which Goldman and Binstock measured their leak currents a 40 mV hyperpolarization should have shut off the n component almost entirely.

The Sodium Conductance

From an examination of the transient current reversal potential as a function of the external sodium concentration, $[Na]_o$, in *Myxicola* Goldman and Binstock (1969 *a*) concluded that the transient current is carried largely by sodium ions, and that the transient channels in *Myxicola* seem to be more selective than those of the squid axons studied by Chandler and Meves

(1965). The transient current and conductance are referred to as I_{Na} and g_{Na}, respectively. Fig. 8 shows peak g_{Na} relative to the maximum value for that axon, g_{Namax}, as a function of membrane potential. Data from the same five axons on which the g_K observations were made are shown, and individual g_{Namax} values are tabulated in Table I. V_{Na}'s were determined from the zero current potential of the corrected currents (see Methods) and are also tabulated in Table I. Mean V_{Na} in these axons is slightly less than in the more extensive series studied by Goldman and Binstock (1969 *a*). The solid line indicates an *e*-fold increase in g_{Na} for 12 mV.

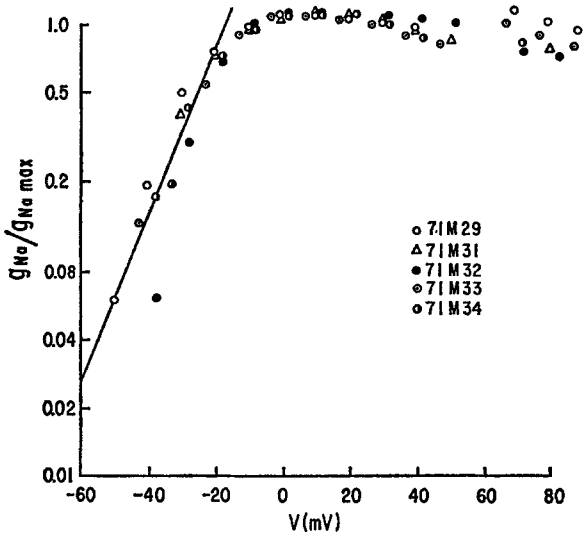

FIGURE 8. Peak sodium conductance relative to the maximum value in each axon, g_{Na}/g_{Namax}, as a function of membrane potential in *Myxicola*. Each symbol type represents a different axon. The solid line has been drawn to show an *e*-fold change in conductance for 12 mV. Axon 71M31 was held at its natural resting potential. All others were conditioned with a 50 mV hyperpolarizing step for 80 ms.

g_{Na} as a function of potential and time was again analyzed as described by Hodgkin and Huxley (1952 *c*). g_{Na} was assumed to be proportional to the product of h and some power of m, where h and m are defined by expressions analogous to Eq. 1. In the potential range where g_{Na} is equal to g_{Namax} the steady-state value of m, m_∞, was assumed to be unity. For potential steps in this range the exponential decay of the g_{Na} when extrapolated to the beginning of the step gives $\overline{g_{Na}}\, h_o$ where $\overline{g_{Na}}$ is the proportionality constant and h_o is the initial value of h. h_o values were taken from Goldman and Schauf (1972).

The points in Fig. 9 are experimental values of g_{Na}, from a single axon, as a function of time for each of the potentials indicated at the right. The solid

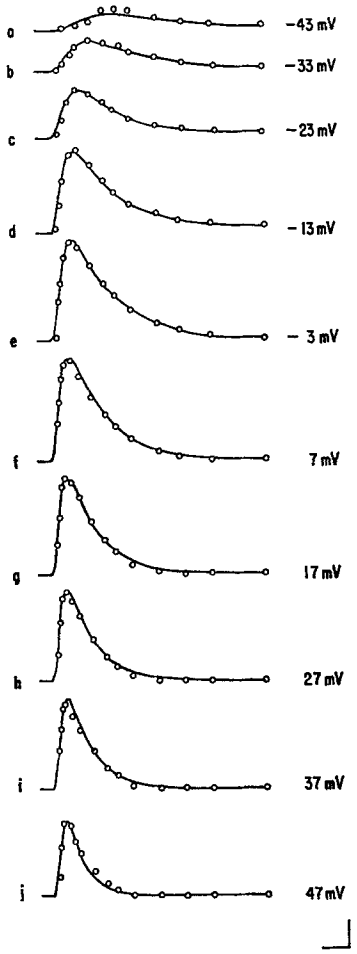

FIGURE 9. Sodium conductance as a function of time for each of the potentials indicated. The circles are experimental values and the solid lines have been computed according to $g_{Na} = \overline{g_{Na}} m^3 h$ (see text). The horizontal lines at the left indicate zero conductance. Scale: (*a*), (*b*), 3 mmho/cm², (*c*)–(*j*), 5 mmho/cm², 1 ms.

curves, which are taken to be a good description of the points, have been computed from

$$g_{Na} = \overline{g_{Na}} m^3 h, \tag{6}$$

by fitting in succession to the data the expressions

$$h = h_\infty - (h_\infty - h_o) e^{-t/\tau_h} \tag{7}$$

and

$$m = m_\infty - (m_\infty - m_o) e^{-t/\tau_m}. \tag{8}$$

The time constants and steady-state values are related to the respective rate constants as described for g_K. A power of 3 for m was used as 2 gave too little initial delay and 4 was very little different from 3. The horizontal lines at the left of each curve indicate zero conductance for reference. Individual values used to compute each of the curves in Fig. 9 are listed in Table III, and the $\overline{g_{Na}}$ values in Table I.

Fig. 10 shows the collected m_∞ values from each of the five axons analyzed as a function of membrane potential, and Fig. 11 the corresponding τ_m data. The extracted rate constants, α_m (open circles) and β_m (filled circles), are

TABLE III

CONSTANTS USED TO COMPUTE THE g_{Na} CURVES OF FIG. 9

V	m_∞	τ_m	α_m	β_m	h_∞	τ_h	β_h
mV		*ms*	ms^{-1}	ms^{-1}		*ms*	ms^{-1}
−43	0.569	1.155	0.493	0.373	0.0	2.58	0.388
−33	0.594	0.577	1.029	0.704	0.0	2.35	0.426
−23	0.905	0.481	1.881	0.198	0.04	1.27	0.755
−13	0.934	0.330	2.83	0.200	0.024	1.63	0.599
−3	1.0	0.294	3.40	0.0	0.0	1.55	0.645
7	1.0	0.232	4.31	0.0	0.0	1.32	0.758
17	1.0	0.208	4.81	0.0	0.0	1.08	0.926
27	1.0	0.207	4.83	0.0	0.0	0.94	1.064
37	0.99	0.192	5.20	0.05	0.0	0.89	1.124
47	1.0	0.188	5.32	0.0	0.0	0.63	1.587

$\overline{g_{Na}}$ is 38 mmho/cm^2.

shown in Fig. 12. The solid lines in Fig. 12 have been drawn according to

$$\alpha_m = \frac{0.066(V + 45)}{1 - \exp[(V + 45)/5.95]} \tag{9}$$

and

$$\beta_m = 0.075 \exp(-V/23.8). \tag{10}$$

The solid curves in Figs. 10 and 11 have also been computed from Eqs. 9 and 10.

h parameters fitted to the g_{Na} curves are shown in Figs. 13 through 15. Over the range of −120 to about −5 mV there are also data available on inactivation parameters for *Myxicola* axons, determined from the effects of conditioning pulses of various potentials and durations on the peak I_{Na} produced by a fixed test pulse (Goldman and Schauf, 1972). This provides a range of about 45 mV over which τ_h and also h_∞ values determined by the two methods may be compared.

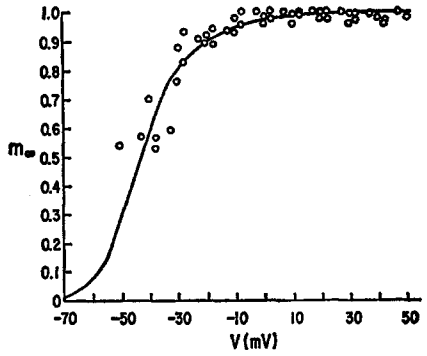

FIGURE 01

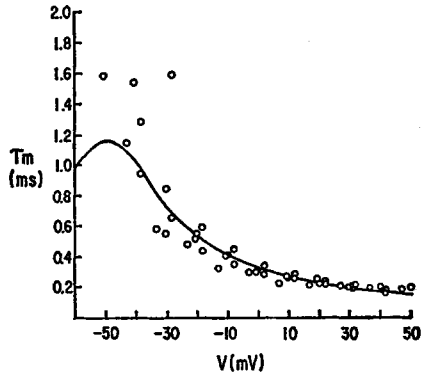

FIGURE 11

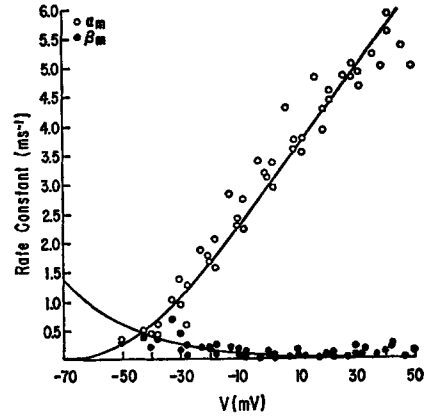

FIGURE 12

FIGURE 10. Steady-state value of the sodium activation variable, m_∞, as a function of membrane potential. The solid curve has been computed from Eqs. 9 and 10 in the text.
FIGURE 11. The time constant of the sodium activation variable, τ_m, as a function of membrane potential. The solid curve has been computed from Eqs. 9 and 10 in the text.
FIGURE 12. Rate constants for the sodium activation variable α_m (open circles) and β_m (filled circles) as functions of membrane potential. The solid curves have been computed from Eqs. 9 (open circles) and 10 (filled circles) in the text.

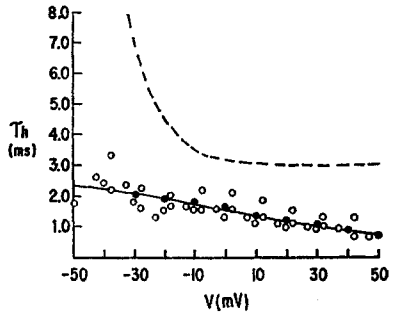

FIGURE 13

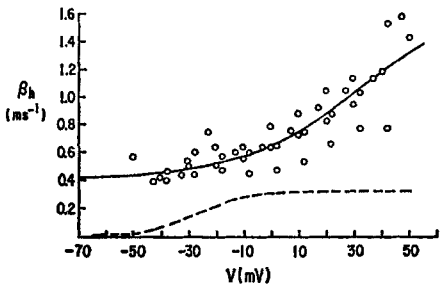

FIGURE 14

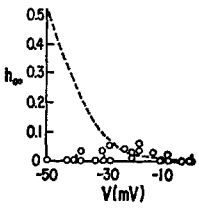

FIGURE 15

FIGURE 13. The time constant of inactivation, τ_h, as a function of membrane potential. The filled circles are from axon 71M31. The solid curve has been drawn from Eq. 12 and the dashed curve from Eqs. 13 and 14 in the text. The dashed curve indicates τ_h values as determined from the effects of conditioning pulses.

FIGURE 14. The inactivation rate constant, β_h, as a function of membrane potential. The solid curve has been drawn from Eq. 12 and the dashed curve from Eq. 14 in the text. The dashed curve indicates β_h values as determined from the effects of conditioning pulses.

FIGURE 15. The steady-state level of the inactivation variable, h_∞, as a function of membrane potential. The dashed curve has been drawn from Eq. 11 and represents the values determined with conditioning pulses. The circles have been fitted to the decay of the sodium conductance during a test pulse.

In the earlier inactivation studies on *Myxicola*, test pulses were always selected from a saturated region of the g_{Na}-voltage curve. h_∞ values, then, are operationally well defined, i.e. they are at their limiting (high) values. In each of the seven axons for which limiting values h_∞ (V) curves were measured, the data could be well described by the expression (Hodgkin and Huxley, 1952 *b*)

$$h_\infty = \frac{1}{1 + \exp(V_h - V/k_h)}, \qquad (11)$$

with one V_h (the potential at which $h_\infty = 0.5$) of -48.5 mV and one k_h (a shape parameter) of -7.9 mV. The rather broad range of variation in V_h values observed in the node by Frankenhaeuser (1959) may at least in part reflect genuine individual variation (Frankenhaeuser and Vallbo, 1965), but perhaps is also a consequence of selecting test pulses from the peak of the $I_{Na}(V)$ characteristic.

It was not possible to demonstrate any clear dependency of τ_h on the test pulse (Goldman and Schauf, unpublished observations). When examined in three axons any effects of changing g_{Na} during the test pulse were within the variance in τ_h measurements. Therefore, although experimental determinations are quite reproducible, the "correct" values for α_h are not known, nor

can they be from this method. However, the values for τ_h (and for β_h for potentials more positive than about -35 to -40 mV) are defined.

The points in Fig. 13 show the τ_h values fitted to the decay of the g_{Na} as a function of membrane potential. The filled circles are from the single axon for which the holding potential was the natural resting potential (-61 mV in this case), the others were obtained with a conditioning step of -50 mV for 80 ms (see Methods). Conditioning hyperpolarization has no effect on τ_h over this range. The solid curve has been computed from Eq. 12,

$$\beta_h = \frac{1}{0.714[\exp(V - 34/-23) + 1]} + 0.4. \tag{12}$$

The dashed curve has been computed from the α_h and β_h functions of Goldman and Schauf (1972),

$$\alpha_c = 0.0051 \exp(-V/31.4) \tag{13}$$

and

$$\beta_c = \frac{1}{3[\exp(V + 25.5/-9.2) + 1]}. \tag{14}$$

The terms α_c and β_c have been used in Eqs. 13 and 14 to distinguish the values determined with conditioning pulses from those fitted to the decay of the g_{Na}.

The dashed curve does not fit the points in Fig. 13. The discrepancy is not due simply to scaling or to a translation along the V axis, and is much greater than the variance in the measurements. τ_h values determined from the effects of conditioning pulses on the peak I_{Na} are not the same as those fitted to the decay of the g_{Na} when compared at the same potential. These results suggest that the process studied by the effects of changes in the initial conditions is not identical to that governing the shutoff of the g_{Na} during a continuous test pulse, and are inconsistent with Hodgkin-Huxley kinetics.

Fig. 14 shows β_h as a function of membrane potential. The solid curve has been computed from Eq. 12 and the dashed curve (β_c) from Eq. 14. Again, the dashed curve does not fit the points. The β_h function fitted to the points differs from those reported in squid (Hodgkin and Huxley, 1952 *c*) and node (Frankenhaeuser, 1960) in that it does not approach zero near the resting membrane potential. This difference arises primarily because we have not made reference to conditioning pulse values in constructing the *Myxicola* β_h function, while those in squid and node have been fitted to values obtained both from the effects of initial conditions and from the decay of the g_{Na} (Hodgkin and Huxley, 1952 *c*; Frankenhaeuser, 1960). Similarly, if overlapping β_h and β_c values had not been available for *Myxicola* a single smooth β_h function lying on the solid curve at positive potentials and on the dashed curve near

the resting membrane potential could have been fitted to the pooled β_h and β_c points.

A comparison of h_∞ values determined by the two methods also yields information on models for the sodium conductance. The points in Fig. 15 indicate the h_∞ values fitted to the decay of the g_{Na} and the dashed line has been computed from Eq. 11. As discussed above, h_∞ (V) curves determined from the effects of conditioning pulses are not uniquely defined. However, the data of Fig. 15 are interesting in that they indicate that there is a 10–20 mV range of conditioning potentials which for *some* range of test pulse potentials will produce the following sequence: The I_{Na} during the conditioning pulse will rise up and then shut off entirely or nearly so (i.e. h will be very near zero). However, during the immediately following (more depolarizing) test pulse a large I_{Na} will be observed, which will again inactivate entirely. These results indicate that the inactivation of the I_{Na} is not governed by the h variable of Hodgkin and Huxley, i.e. is not caused by the monotonic decrease of some variable under a depolarizing potential step, and that the g_{Na} is not determined by the product of two independent first order variables.

There is really little disagreement between our data and that of previous workers. New conclusions have been developed because we had an extensive range of overlapping values which were not previously available. Hodgkin and Huxley (1952 *b,c*) did present a few such overlapping values, but they were sparse and widely scattered. Overall the only difference we find between our data and that of Hodgkin and Huxley is that the I_{Na} in *Myxicola* inactivates completely or nearly so at every test potential. We have never seen sodium currents that inactivate partially or not at all, as they have described for small depolarizing steps.

Computed Action Potentials

In this section we present computations of action potentials and subthreshold responses based on the data determined in this paper and by Goldman and Schauf (1972). Computations were first done using only the parameters obtained in this paper, i.e., obtained from the currents recorded in response to a series of potential steps with fixed initial conditions. We refer to this set of parameters as the five parameter model, as α_h was taken as zero throughout (Fig. 15). An h_o of 0.9 was introduced as a constant.

Computations were made of membrane action potentials (Hodgkin and Huxley, 1952 *c*). The system of equations to be solved is:

$$I_M = C_M dV_d/dt + \overline{g_{Na}}\, m^3 h(V_d - V_{d\,Na}) + \overline{g_K} n^2(V_d - V_{d\,K}) + g_L(V_d - V_{d\,L}), \quad (15)$$

$$dm/dt = \alpha_m(1 - m) - \beta_m m, \quad (16)$$

$$dn/dt = \alpha_n(1 - n) - \beta_n n, \quad (1)$$

$$dh/dt = \alpha_h(1 - h) - \beta_h h. \tag{17}$$

where V_d, the membrane potential as displacement from rest, is given by

$$V_d = V + 65.$$

C_M is the membrane capacitance, and I_M is the total membrane current. Expressions for α_n, β_n, α_m, β_m, and β_h are given above (Eqs. 4, 5, 9, 10, and 12, respectively). The condition that I_M equals the stimulating current for the duration of a stimulating pulse and is zero for all other times completes the equation system.

Constants used in the computation are listed in Table IV. C_M was determined from an earlier series of eight axons by integrating the current under the capacitative surge (range: 0.62 to 0.85 μF/cm^2; Goldman and Binstock, unpublished observations). h_o was taken from Goldman and Schauf (1972), and m_o and n_o from Figs. 10 and 3. V_{dL} is the value needed to make the total membrane current zero at rest. All other values have been rounded off from the means of the experimental determinations in Table I. Computations were made using a forth order Runge-Kutta with automatic adjustment of step size.

TABLE IV

CONSTANTS USED FOR THE COMPUTATION OF ACTION POTENTIALS

Term	Value
C_M	0.75 μF/cm^2
$\overline{g_{Na}}$	40 mmho/cm^2
$V_{d\,Na}$	125 mV
$\overline{g_K}$	8 mmho/cm^2
$V_{d\,K}$	−13 mV
g_L	0.6 mmho/cm^2
$V_{d\,L}$	1.253 mV
m_o	0.04
n_o	0.10
h_o	0.90

In Fig. 16 *a* a computed (five parameter) action potential is shown, and Fig 16 *c* shows an experimental membrane action potential from *Myxicola*. The computed action potential generally resembles the experimental in form and amplitude, with the same sort of differences as between other computed and experimental action potentials (i.e. the peak is too sharp and the base too broad in the computed response). In Figs. 17 to 19 (solid curves) the computed time-courses of g_{Na}, g_K, m, n, h, I_{Na}, I_K, and I_L during an action potential are shown. These curves are quite similar to the corresponding computed functions in squid and node (Hodgkin and Huxley, 1952 *c*; Frankenhaeuser and Huxley, 1964).

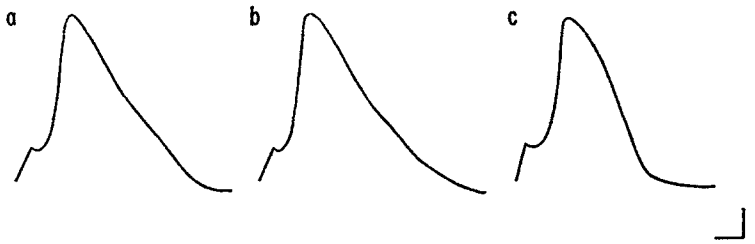

FIGURE 16. Action potentials in *Myxicola*. (*c*) is an experimental record and (*a*) (five parameter model) and (*b*) (expanded model) have been computed as described in the text. The stimulus was a 0.5 ms current pulse of 0.04 mA/cm² in both (*a*) and (*b*). Scale: 20 mV, 1 ms.

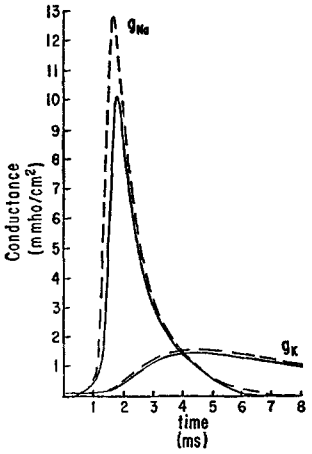

FIGURE 17

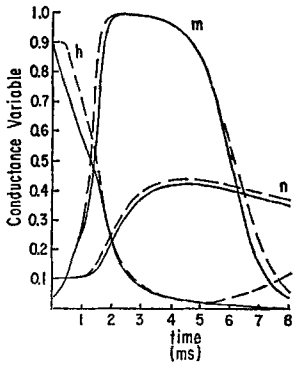

FIGURE 18

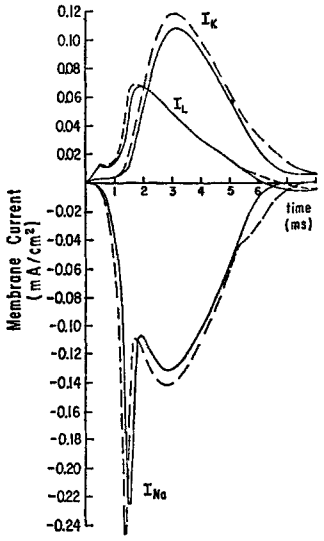

FIGURE 19

FIGURE 17. Computed sodium and potassium conductance as a function of time during an action potential. Solid curves are for the five parameter model and the dashed curves are for the expanded model.

FIGURE 18. Computed time-course of the conductance variables during an action potential. The solid curves are for the five parameter model and the dashed curves are for the expanded model.

FIGURE 19. Computed time-course of the sodium, potassium, and leak currents during an action potential. Solid curves are for the five parameter and the dashed curves for the expanded model.

Computed responses to a series of brief current pulses of increasing intensity agreed closely with the behavior of real axons, including the presence of a threshold. No effort was made to define threshold current very precisely. However, a 0.5 ms current pulse of 0.03 mA/cm² produced an action potential, while an 0.027 mA/cm² pulse produced only a subthreshold response. Subthreshold oscillations in response to long current pulses (Hodgkin and Hux-

ley, 1952 *c*) are not observed experimentally in *Myxicola* (Fig. 20 *b*). Correspondingly, they are not seen in computed responses either (Fig. 20 *a*).

Much of the normal electrical behavior of an axon can be simulated from the five parameter model. However, phenomena related to recovery, e.g., refractoriness, presence of repetitive discharges, postanodal excitation, etc., cannot be accounted for without making reference to *both* the β_c and α_c data obtained with various conditioning pulses. Recovery is still not obtained if only the α_c function is substituted for α_h. The action potential shown in Fig. 16 *b* and the dashed curves in Figs. 17 to 19 have been computed as described for the five parameter model except that for V less than -45 mV α_h is set equal to α_c and β_h is set equal to β_c (Eqs. 13 and 14).

The response for this expanded model in Fig. 16 *b* is quite similar to that shown in Fig. 16 *a*. There are small differences as expected from the fact that h

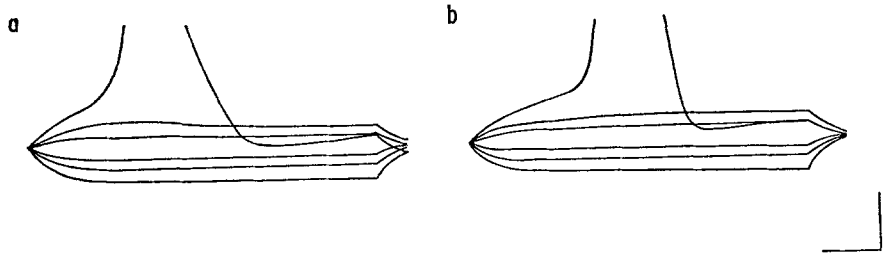

FIGURE 20. (*a*), computed responses (five parameter model) and (*b*), experimental responses to long current pulses. Scale: 20 mV, 2.5 ms.

does not decline as quickly (Fig. 18) for the action potential of Fig. 16 *b*, i.e., the threshold is lower, the rise of the action potential is somewhat faster, and the amplitude slightly greater. However, if α_h and β_h are set equal to α_c and β_c for V less than -15 mV, greatly prolonged action potentials are produced. The changes in g_{Na}, g_K, m, n, and the membrane currents (Figs. 17 to 19, dashed curves) are consistent with an action potential rising more quickly to a higher potential. The break in the decline of I_{Na} at about 5.5 ms (Fig. 19 lower dashed curve) is a consequence of the rather artificial way that α_c and β_c have been introduced. Subthreshold behavior is also similar for the expanded model except that threshold is lower (a 0.5 ms pulse at 0.02 mA/cm^2 produced an action potential, a 0.018 mA/cm^2 pulse did not). As for the five parameter model, subthreshold oscillations were not seen.

An important difference between this expanded model and the five parameter model is that h will increase again at the termination of the action potential (Fig. 18). Fig. 21 *a* shows the time-course of refractoriness computed from the expanded model. No effort was made to define the limits of the absolute refractory period, rather a 0.5 ms current pulse at a fixed intensity of 0.07 mA/cm^2 was applied at various times. A set of experimental records is shown

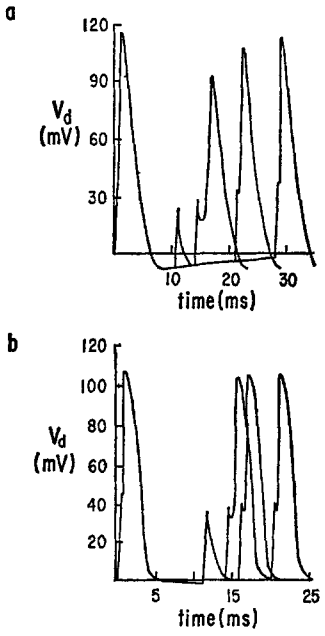

FIGURE 21. Computed (*a*) and experimental (*b*) time-course of refractoriness. The stimulus was a constant 0.5 ms pulse of 0.07 mA/cm² (about 3.5 times threshold) in (*a*) and a constant 0.5 ms pulse of about twice threshold in (*b*).

in Fig. 21 *b*. There is general agreement except that the computed responses recover more gradually. The expanded model produced repetitive discharges as a response to a maintained current pulse. However, we have never observed repetitive discharges experimentally in *Myxicola*.

Frankenhaeuser and Vallbo (1965) presented a useful series of computations based on the Frankenhaeuser-Huxley equations. They showed that these equations could be converted from a form in which only a single action potential would be produced as a response to a maintained current pulse to one in which trains of action potentials would be produced indefinitely, by simply translating the α_h function by 3 mV along the voltage axis. The position of the α_h function along the V axis is of course much affected by the position of the h_∞ curve along the V axis. It seems difficult therefore to attach much significance to the presence or absence of repetitive discharges computed from Hodgkin-Huxley type equations, or to any computed phenomena very dependent on α_h.

The results of our computations may be summarized as follows. From one type of voltage-clamp experiment (a series of steps to different depolarizing potentials with fixed initial conditions) one can obtain data which account for many of the major features of electrical behavior of axons: the form and

amplitude of the action potential, undershooting afterpotentials, the presence of a threshold, and normal subthreshold behavior. All the data needed to account for recovery phenomena (i.e. the time-course of refractoriness, repetitive action potentials), come from a different type of voltage-clamp experiment, an examination of the effects of changes in initial conditions on clamp currents. However, inactivation parameters taken only from this second type of experiment cannot produce a normal action potential. The different inactivation parameters, then, arise from different sorts of experiments and seem to account for different phenomena. It is interesting to note that all of the available evidence bearing on the question of coupled vs. independent activation-inactivation kinetics for the sodium conductance comes from experiments relating to recovery phenomena.

DISCUSSION

Several points of interest may be raised from these data. g_{Na} and g_K increase with voltage at rates up to 12 and 13 mV for an *e*-fold change in conductance. These values indicate a voltage sensitivity of the excitable channels in *Myxicola* some 2–3 times less than in squid (Hodgkin and Huxley, 1952 *a*), and are consistent with a gating process in which only two charged particles cross the membrane.

To account for the delay in the development in g_K in squid, observed in the presence of strong conditioning hyperpolarization, n must be raised to the 25th power (Cole and Moore, 1960 *b*). A power this high seems difficult to interpret as a number of cooperatively moving particles and implies that the power to which n is raised should probably be viewed as a formal parameter rather than as a physically interpretable number. Our data tend to support this view. The difference between n^2 for *Myxicola* and node (Frankenhaeuser, 1963) and n^4 for squid, which apply in the absence of conditioning polarization, does not seem to be very important. However, the difference between 25 for squid and 3 for the maximum effect in *Myxicola*, in the presence of strong conditioning hyperpolarization, seems too great to dismiss. Attaching a mechanistic significance to these powers would imply that the g_K processes in squid and *Myxicola* are quite different. A more likely interpretation would seem to be that the behavior of the n variable only approximately describes the physical process governing the potassium conductance.

Much more serious questions may be raised regarding the m and h variables of Hodgkin and Huxley. When compared at the same potential, τ_h as determined from the decay of the g_{Na} during a test pulse is different from that determined from the effects of conditioning potentials of different durations on the peak I_{Na} produced by a fixed test pulse. The process studied by the effects of changes in initial conditions, then, is not identical to that producing the shutoff of the g_{Na} during any test pulse, as is required in the Hodgkin-Huxley

scheme. For durations of the conditioning pulse long relative to τ_m, the effects of further increases in conditioning pulse duration should have been determined entirely by changes in h_o. That they are not, indicates that the g_{Na} is not governed by Hodgkin and Huxley's m and h variables. If the g_{Na} is determined by a second order variable, there is no general requirement that the time constants determined by the two different methods be the same.

Another question is raised by the data of Fig. 15. These data indicate that there is a range of conditioning pulse potentials during which I_{Na} will eventually shut off entirely, i.e. h will go to zero, and for which there will still be substantial I_{Na} (which again inactivates entirely) produced during the immediately following test pulse. These data are inconsistent with an inactivation variable which is a monotonic function of potential, and of time at any fixed potential; and moreover indicate that the g_{Na} is not determined by the product of two independent first order variables.

These results, together with those of Goldman and Schauf (1972) and Hoyt and Adelman (1970), describe an expanded array of behaviors of the sodium inactivation process, and should be helpful in defining models for the sodium conductance. One view (of many) qualitatively consistent with all of these results is that the sodium conductance is governed by a single, second order variable.

Hoyt (1968) has computed shifts of the steady-state inactivation curve with changing test pulses, and Moore and Jakobsson (1971) have computed delays in the inactivation-time curve, both from coupled activation-inactivation models. Chandler and Meves (1970) have described a variety of inactivation phenomena in squid axons internally perfused with NaF. For example, they found that the time-course of the reactivation curve was not monotonic. They were also able to quantitatively account for their observations in terms of a coupled activation-inactivation model. However, they assumed in addition an independent Hodgkin-Huxley m process.

Jakobsson and Moore (1971) and Moore and Jakobsson (1971) have claimed that shifts in the h_∞ curve with changing test pulses are not predictable from a generalized second order coupled model, and that Hoyt's (1968) computed shifts arise from some other feature of her equations. These conclusions seem to have been based on a single numerical computation from their equations in which h_∞ curves computed for test pulses to 30 and to -30 mV were compared. No difference was detected (their Fig. 5). However Moore and Jakobsson may not have selected test pulses appropriately for this comparison. Goldman and Schauf (1972) were able to describe their somewhat limited range of data on h_∞ shifts with the expression

$$\Delta V_h = 5.8\, g_{Na_2}/g_{Na_1} - 5.8, \tag{18}$$

where ΔV_h is the difference, in millivolts, in V_h values from two h_∞ curves determined with test pulses having peak sodium conductances g_{Na_1} and g_{Na_2}.

Using Moore and Jakobsson's test pulse potentials, a value for g_{Na_2}/g_{Na_1} of about 1.3 may be estimated from their Fig. 3. From Eq. 18 we get a ΔV_h of only 1.7 mV, which would not be detectable in their Fig. 5. Their conclusion, therefore, that h_∞ shifts are not a general feature of coupled models does not seem justified.

Several simple alternative models are ruled out by the array of data discussed above. For example, it cannot be that Hodgkin and Huxley's h is itself determined by the product of two independent first order variables of differing time constants, as proposed by Haas, Kern, Einwachter, and Tarr (1971) for frog atria. In that case inactivation as determined by either method should not be a simple exponential in *Myxicola* in contrast to the experimental observations. Moreover, neither the data of Fig. 15 or the observations of Goldman and Schauf (1972) would be accounted for. Another model consisting of three independent first order variables was discussed by Chandler and Meves (1970). In their model

$$g_{Na} = \overline{g_{Na}}\, m^3\, (h_1 + h_2), \tag{19}$$

where m is the Hodgkin-Huxley m, h_1 is like the Hodgkin-Huxley h and h_2 is another activation variable, i.e., it (and consequently g_{Na}) increases on a depolarizing step. This model would account for the data of Fig. 15 except that the I_{Na} during the test pulse should not not inactivate at all. Moreover, neither the two sets of values for τ_h nor the simple translation of h_∞ curves along the V axis with changing test pulses are accounted for. Another way to account for the data of Fig. 15 is to suppose that activation and inactivation are independent, but that only those channels which are activated and inactivated during the conditioning pulse will be found to be inactivated during the test pulse. However, the steady-state inactivation curve for any test pulse cannot be constructed from the data of Fig. 8 as would be required, and again the different τ_h values would not be accounted for.

Parameters in terms of a coupled activation-inactivation scheme have not yet been extracted for *Myxicola* axons. Until they are available it is not clear to what extent the sodium conductance can be described in terms of a single second order variable, as first proposed by Hodgkin and Huxley (1952 *c*).

We thank Miss Shirlene Showell for valuable technical assistance and Mr. Gerald Ebert for assistance with the electrophysiological observations. We also thank Doctors R. C. Hoyt, H. Lecar, and L. J. Mullins for reading the manuscript.

This work was supported in part by U. S. Public Health Service Research Grant NS 07734.

Received for publication 28 August 1972.

BIBLIOGRAPHY

ARMSTRONG, C. M. 1970. Comparison of g_k inactivation caused by quaternary ammonium ion with g_{Na} inactivation. *Biophys. Soc. Annu. Meet. Abstr.* **10**:185 *a*.

BINSTOCK, L., and L. GOLDMAN. 1969. Current and voltage-clamped studies on *Myxicola* giant axons; effect of tetrodotoxin. *J. Gen. Physiol.* **54**:730.

BINSTOCK, L., and L. GOLDMAN. 1971. Rectification in instantaneous potassium current voltage relations in *Myxicola* giant axons. *J. Physiol. (Lond.)*. **217**:517.

CHANDLER, W. K., and H. MEVES. 1965. Voltage clamp experiments on internally perfused giant axons. *J. Physiol. (Lond.)*. **180**:788.

CHANDLER, W. K., and H. MEVES. 1970. Evidence for two types of sodium conductance in axons perfused with sodium fluoride solution. *J. Physiol. (Lond.)*. **211**:653.

COLE, K. S., and J. W. MOORE. 1960 *a*. Liquid junction and membrane potentials of the squid giant axon. *J. Gen. Physiol.* **43**:971.

COLE, K. S., and J. W. MOORE. 1960 *b*. Potassium ion current in the squid giant axon: dynamic characteristic. *Biophys. J.* **1**:1.

FRANKENHAEUSER, B. 1959. Steady state inactivation of sodium permeability in myelinated nerve fibers of *Xenopus laevis*. *J. Physiol. (Lond.)*. **148**:671.

FRANKENHAEUSER, B. 1960. Quantitative description of sodium currents in myelinated nerve fibers of *Xenopus laevis*. *J. Physiol. (Lond.)*. **151**:491.

FRANKENHAEUSER, B. 1963. A quantitative description of potassium currents in myelinated nerve fibers of *Xenopus laevis*. *J. Physiol. (Lond.)*. **169**:424.

FRANKENHAEUSER, B., and A. L. HODGKIN. 1957. The action of calcium on the electrical properties of squid axons. *J. Physiol. (Lond.)*. **137**:218.

FRANKENHAEUSER, B., and A. F. HUXLEY. 1964. The action potential in the myelinated nerve fiber of *Xenopus laevis* as computed on the basis of voltage clamp data. *J. Physiol. (Lond.)*.

FRANKENHAEUSER, B., and A. B. VALLBO. 1965. Accommodation in myelinated nerve fibers of *Xenopus laevis* as computed on the basis of voltage clamp data. *Acta Physiol. Scand.* **63**:1. **171**: 302.

GOLDMAN, D. E. 1943. Potential, impedance and rectification in membranes. *J. Gen. Physiol.* **27**:37.

GOLDMAN, L., and L. BINSTOCK. 1969 *a*. Current separations in *Myxicola* giant axons. *J. Gen. Physiol.* **54**:741.

GOLDMAN, L., and L. BINSTOCK. 1969 *b*. Leak current rectification in *Myxicola* giant axons; constant field and constant conductance components. *J. Gen. Physiol.* **54**:755.

GOLDMAN, L., and C. L. SCHAUF. 1972. Inactivation of the sodium current in *Myxicola* giant axons; evidence for coupling to the activation process. *J. Gen. Physiol.* **59**:659.

HAAS, H. G., R. KERN, H. M. EINWACHTER, and M. TARR. 1971. Kinetics of Na inactivation in frog atria. *Pfluegers Arch. Eur. J. Physiol.* **323**:141.

HODGKIN, A. L., and A. F. HUXLEY. 1952 *a*. Currents carried by sodium and potassium ions through the membrane of the giant axon of *Loligo*. *J. Physiol. (Lond.)*. **116**:449.

HODGKIN, A. L., and A. F. HUXLEY. 1952 *b*. The dual effect of membrane potential on sodium conductance in the giant axon of *Loligo*. *J. Physiol. (Lond.)*. **116**:497.

HODGKIN, A. L., and A. F. HUXLEY. 1952 *c*. A quantitative description of membrane current and its applications to conduction and excitation in nerve. *J. Physiol. (Lond.)*. **117**:500.

HODGKIN, A. L., A. F. HUXLEY, and B. KATZ. 1952. Measurement of current voltage relations in the membrane of the giant axon of *Loligo*. *J. Physiol. (Lond.)*. **116**:424.

HODGKIN, A. L., and B. KATZ. 1949. The effect of sodium ions on the electrical activity of the giant axon of the squid. *J. Physiol. (Lond.)*. **108**:37.

HOYT, R. C. 1963. The squid giant axon; mathematical models. *Biophys. J.* **3**:399.

HOYT, R. C. 1968. Sodium inactivation in nerve fibers. *Biophys. J.* **8**:1074.

HOYT, R. C., and W. J. ADELMAN. 1970. Sodium inactivation; experimental test of two models. *Biophys. J.* **10**:610.

JAKOBSSON, E., and L. E. MOORE. 1971. On making models of the sodium inactivation of axonal membranes. *Biophys. J.* **11**:385.

MOORE, L. E., and E. JAKOBSSON. 1971. Interpretation of the sodium permeability changes of myelinated nerve in terms of linear relaxation theory. *J. Theor. Biol.* **33**:77.